PROCEEDINGS OF SCIENCE

# Energy dependence of nuclear effects in hadron-nucleus collisions

**K. Tywoniuk***, **I. C. Arsene, L. Bravina and E. Zabrodin**
*University of Oslo*
*E-mail:* konrad.tywoniuk@fys.uio.no

**A. B. Kaidalov**
*ITEP, Moscow*

The energy dependence of light and heavy particle production in hadron-nucleus collisions is discussed. Whereas the production mechanism at lower energies can be understood in the Glauber rescattering picture, experimental data at RHIC indicate that particles are mostly produced in coherent processes. The importance of energy-momentum conservation is shown to be crucial at forward rapidities for the whole energy range. We also discuss the behaviour of $\alpha(x_F)$ with energy for light particles and $J/\psi$. Finally, we make predictions for the future LHC experiment.

*High-pT physics at LHC*
*March 23-27 2007*
*University of Jyväskylä, Jyväskylä, Finland*

*Speaker.

 

PoS(LHC07)035

## 1. Introduction

In addition to being an important tool for modeling nucleus-nucleus collisions (AA), proton-nucleus (pA) collisions are also interesting by themselves as they probe nuclear effects related to multiple scattering and possible hadronization in nuclear matter. The origin of these effects is still under debate. In recent years most of theoretical activity has focused on novel high-energy nuclear effects, such as parton saturation, yet it seems that past and present energies (RHIC) do not provide enough phase space for these effects to appear. It will be our task in this paper to review some well-known low-energy models and to introduce high-energy effects (shadowing) to describe data on light and heavy particles in pA collisions in the energy range $\sqrt{s} = 17.3 - 5500$ GeV.

Our starting point is noticing that a significant change in the underlying dynamics of a hadron-nucleus collision takes place with growing energy of the incoming particles. At low energies, the total cross section is well described within the probabilistic Glauber model [1]. In the reggeon approach these interactions are described by so-called planar diagrams depicted in Fig. 1 (left). At higher energies, $E > E_C \sim m_N \mu R_A$ ($\mu$ is a characteristic hadronic scale, $\mu \sim 1$ GeV, and $R_A$ is the radius of the nucleus) corresponding to a coherence length

$$l_C = \frac{1}{2 m_N x} , \tag{1.1}$$

the typical hadronic fluctuation length can become of the order of, or even bigger than, the nuclear radius and there will be coherent interaction of hadron constituents with several nucleons of the nucleus. In this energy range, the contribution from planar diagrams is damped by a factor $\sim 1/E$ [2] and the dominant contribution arises from non-planar diagrams, shown in Fig. 1 (right). The sum of all diagrams was calculated by Gribov [3, 4], who introduced a correction to the Glauber series by taking into account the diffractive intermediate states. The forward hadron-nucleus ($hA$ or $\gamma^* A$) scattering amplitude can then be written as the sum of diagrams shown in Fig. 2, i.e. as

$$\sigma_{\gamma^* A} = A\sigma_{\gamma^* N} + \sigma^{(2)}_{\gamma^* A} + \dots , \tag{1.2}$$

In Eq. (1.2), the first term simply represents the Glauber elastic contribution and subsequent terms describe multiple interactions of the incoming probe with the nucleons in the target nucleus. The space-time picture analogy to the Glauber series is however lost, as the interactions with different nucleons of the nucleus occur nearly simultaneous in time. This phenomenon is related to inelastic shadowing corrections.

An additional effect which comes into play at high energies, is the possibility of interactions between soft partons of the different nucleons in the nucleus. In the Glauber-Gribov theory this

**Figure 1:** Planar (left) and non-planar (right) diagram of multiple scattering. The former decreases as $\sim 1/E$ above the critical energy, the latter is controlled by $t_{min}$ effects.

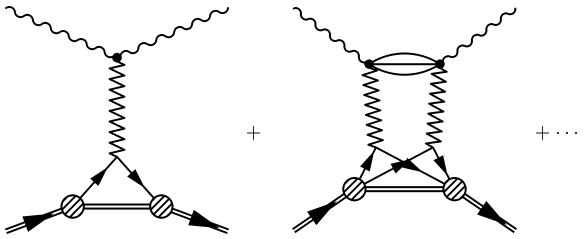

**Figure 2:** Glauber-Gribov series: the single and double scattering contribution to the total $\gamma^* N$ cross section.

corresponds to interactions between Pomerons. The necessity to include such "enhanced" diagrams at high energies can be related to unitarization of all amplitudes. In particular, diagrams involving triple-Pomeron interactions are related to large-mass intermediate states in Fig. 2 which give a dominant contribution to shadowing. There is a connection between these effects and saturation effects in the parton picture.

In pA collisions, nuclear effects are usually discussed in terms of the power-law parameterization

$$\frac{\mathrm{d}\sigma_{pA}}{\mathrm{d}^3 p} = \frac{\mathrm{d}\sigma_{pN}}{\mathrm{d}^3 p} A^{\alpha(x_F)} , \tag{1.3}$$

where $\sigma_{pA}$ ($\sigma_{pN}$) is the inclusive cross section off a nucleus (nucleon). The function $\alpha(x_F)$ characterizes nuclear effects at different longitudinal momentum fractions of the produced particle. For a large range of energies, $\alpha$ exhibits a very interesting scaling in $x_F$ for both light and heavy particle production as seen in Fig. 3. For $J/\psi$, $\alpha(x_F)$ decreases from 0.95 at $x_F \approx 0$ to values $\alpha \sim 0.75$ at $x_F \simeq 0.8$ thus indicating an increase of absorption as $x_F$ increases [5–7]. No scaling in Bjorken $x$ of the nucleus, $x_2$, is observed, indicating breaking of QCD factorization at these energies. The suppression of light particles follow a similar trend. Another striking feature is the rather large suppression of low-energy data at $x_F = 0$. These features are reproduced by models invoking mechanisms of attenuation and/or energy-loss in nuclear matter [8–11].

Recent data from RHIC experiment on charged hadron [12] and $J/\psi$ [13] production in dAu collisions at $\sqrt{s} = 200$ GeV are also shown in Fig. 3 (data from [12] have been integrated over $p_\perp$ between 0.7-1.0 GeV/c). The suppression at $x_F = 0$ is smaller compared to lower energies contrary to the expectation of many theoretical models. Despite the limited kinematics accessible in collider experiments, the RHIC data also hints towards a breaking of $x_F$ scaling.

The behavior of $\alpha(x_F)$ with energy allows a natural explanation within the Gribov theory of multiparticle production described above. At very high energies Abramovsky-Gribov-Kancheli (AGK) cutting rules [15] lead to cancellation of the Glauber-type diagrams in the central rapidity region and only enhanced diagrams, or in other words shadowing of small-$x$ partons, contribute to $\alpha < 1$. Experimental data indicate, that the transition from incoherent to coherent particle production happens at RHIC energies for $J/\psi$ production. In the following we will discuss these trends in more detail and present calculations involving gluon shadowing and effects of energy-momentum conservation.

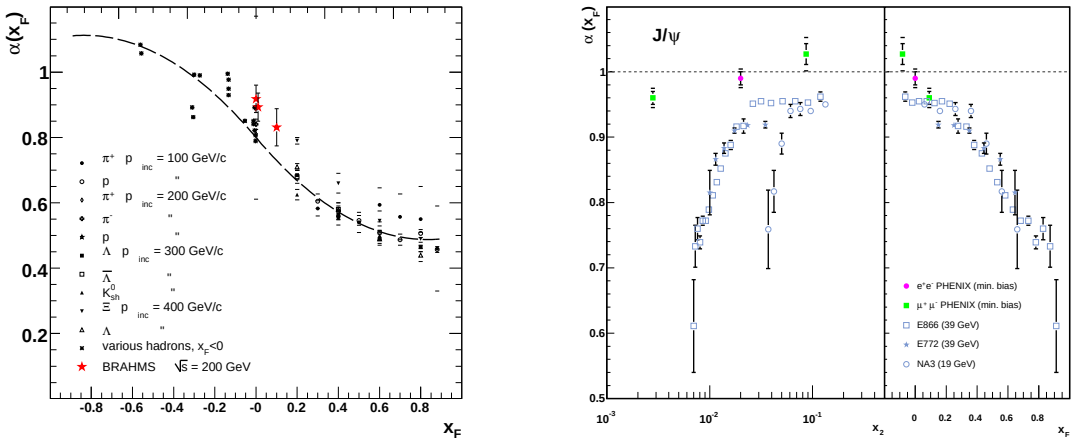


**Figure 3:** $\alpha$ vs. $x_F$ (and $x_2$) in proton-nucleus collisions at different energies for production of light particles (left) and $J/\psi$ (right). Experimental data are taken from [5 – 7, 12 – 14].

## 2. Gribov inelastic shadowing

In the relativistic Gribov theory [3, 4] the collision proceeds through simultaneous interactions of the projectile with nucleons in the nucleus and therefore the intermediate states, shown in Fig. 2, are no longer the same as the initial state. The multiparticle content of the diagrams is given by AGK cutting rules [15], where the intermediate states are on-shell. The cut contribution of the double rescattering diagram can be expressed in terms of diffractive deep inelastic scattering (DDIS). The variable $\beta = \frac{Q^2}{Q^2+M^2} = x/x_{I\!P}$ plays the same role for the Pomeron as the Bjorken variable, $x$, for the nucleon. We assume that the amplitude of the process is purely imaginary. The contribution from the second term in Eq. (1.2) to the total $\gamma^* A$ cross section is given by

$$\sigma^{(2)}_{\gamma^* A} = -4\pi A(A-1)\int \mathrm{d}^2 b \int_{M^2_{min}}^{M^2_{max}} \mathrm{d}M^2 \left[\frac{\mathrm{d}\sigma^{\mathscr{D}}_{\gamma^* N}(Q^2, x_{I\!P}, \beta)}{\mathrm{d}M^2\,\mathrm{d}t}\right]_{t=0} |F_A(q_L, b)|^2 \,, \qquad (2.1)$$

where

$$|F(q_L, b)|^2 = \int_{-\infty}^{\infty} \mathrm{d}z\, \rho_A(b,z)\, e^{iq_L z} \,, \qquad (2.2)$$

is the so-called longitudinal form factor and $q_L = \sqrt{-t_{min}} = m_N x_{I\!P}$ [16].

In Eq. (2.1), $M^2_{min}$ corresponds to the minimal mass of the diffractively produced hadronic system, $M^2_{min} = 4m^2_\pi = 0.08$ GeV$^2$, and $M^2_{max}$ is chosen according to the condition: $x_{I\!P} \leq x^{max}_{I\!P}$. We use the standard choice for $x^{max}_{I\!P} = 0.1$ [17]. It is convenient as it guarantees the disappearance of nuclear shadowing at $x \sim 0.1$ in accord to experimental data.

We are interested in calculating shadowing for small-$x$ quarks and gluons and consider because of this DDIS on nucleons where this information can be extracted. Note that since Eq. (2.1) is obtained under very general assumptions, i. e. analyticity and unitarity, it can be applied for arbitrary values of $Q^2$ provided $x$ is very small [18].

### 2.1 Diffractive gluon distribution

The cross sections of diffractive processes are expressed through structure functions, which are in turn associated with distribution functions of partons in the Pomeron. The relation between the diffractive cross section and the diffractive structure function is given by

$$\left[\frac{\mathrm{d}\sigma^{\mathscr{D}}_{\gamma^* N}(Q^2,x_{I\!P},\beta)}{\mathrm{d}M^2\,\mathrm{d}t}\right]_{t=0} \;=\; \frac{4\pi^2\alpha_{em}B}{Q^2\,(Q^2+M^2)}\,x_{I\!P}\,F^{(3)}_{2\mathscr{D}}(Q^2,x_{I\!P},\beta)$$

Assuming Regge factorization we write the diffractive structure function as

$$F^{(3)}_{2\mathscr{D}}(x_{I\!P},Q^2,\beta) \;=\; f_{I\!P}(x_{I\!P})\,F(\beta,Q^2)\,, \tag{2.3}$$

where the first factor is referred to as the ($t$-integrated) Pomeron flux and the second factor, $F(\beta,Q^2)$, is the Pomeron structure function.

Until recently, the diffractive structure function has been poorly known. In particular, the diffractive gluon density was affected by large uncertainty since it is not measured directly in experiment. Results of new high-precision measurements of the diffractive parton distribution functions (DPDFs) presented by the H1 Collaboration [19, 20] give important constraints to our model of shadowing. Due to the indirect extraction of the diffractive gluon density, $\beta g^{\mathscr{D}}(\beta,Q^2)$, from experimental data, two fits were presented, FIT A and FIT B, reflecting the systematic uncertainty of the procedure. Furthermore, a combined fit to DDIS data and diffractive di-jets [21] results in a curve similar to FIT B yet with a slightly smaller gluon density. For completeness, we also compare the new results with the old H1 parameterization [22] presented in 2002. For details on extracted DPDFs and corresponding Pomeron parameters, $\alpha_{I\!P}(0)$ and $\alpha'_{I\!P}$, we refer the reader to the experimental papers [19, 20].

The gluon distribution is almost a factor of 10 bigger than the quark distribution at the same $Q^2$ for a broad region of $\beta$ [19, 20]. Therefore, in the relevant kinematical range for hadron-nucleus and nucleus-nucleus collisions at RHIC and LHC, the gluon density dominates. In what follows, we will therefore consider structure functions of gluons in nuclei. The first term in Eq. (1.2) is then proportional to $AG_N(x,Q^2)$, while the second rescattering term is correspondingly equal to $-A(A-1)G_N(x,Q^2)\int \mathrm{d}^2b\,T_A^2(b)\,f(x,Q^2)$, where

$$f\left(x,Q^2\right) \;=\; 4\pi\int_x^{x_{I\!P}^{max}} \mathrm{d}x_{I\!P}\,B(x_{I\!P})\,f_{I\!P}(x_{I\!P})\,\frac{\beta g^{\mathscr{D}}(\beta,Q^2)}{G_N(x,Q^2)}\,F_A^2(t_{min})\,, \tag{2.4}$$

with $B(x_{I\!P})$ being the diffractive slope parameter. The gluon distribution of the nucleon, $G_N(x,Q^2)=xg(x,Q^2)$, was taken from the CTEQ6M parameterization [23]. The ratio under the integral in Eq. (2.4) is hence the ratio of gluon density in the Pomeron and in the nucleon.

### 2.2 Models of multiple scattering

The summation of all rescatterings in Eq. (1.2) is model dependent. In writing Eq. (2.4) we have assumed that the following factorization holds

$$|F(q_L,b)|^2 \;=\; T_A^2(b)\,F_A^2\,(t_{min})\;, \tag{2.5}$$

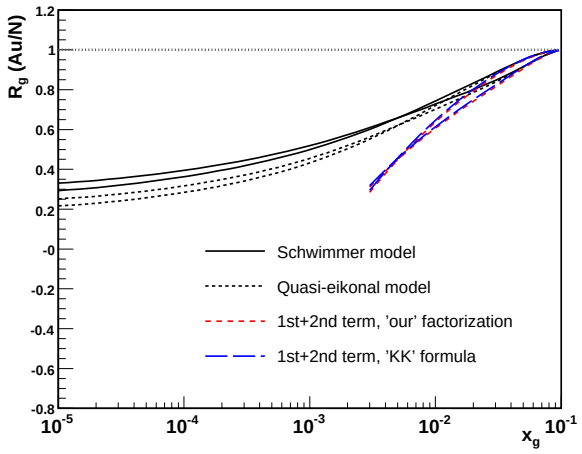


**Figure 4:** Comparison of different models for higher order rescatterings. See text for details.

where $T_A(b) = \int_{-\infty}^{+\infty} \mathrm{d}z\, \rho_A(b,z)$ is the nuclear density profile and $F_A$ is given by

$$F_A(t_{min}) \;=\; \int \mathrm{d}^2 b\, J_0(\sqrt{-t_{min}}b)\, T_A(b)\;. \tag{2.6}$$

Here $J_0(x)$ denotes the Bessel function of the first kind. Equation (2.5) is an identity for nuclear densities which depend separately on $b$ and $z$, however we have checked that calculations with a Woods-Saxon nuclear density profile lead to negligible corrections to the exact expression. For consistency, we show calculations of $(\sigma^{(1)}+\sigma^{(2)})/\sigma_{\gamma^* N}$ in Fig. 4 where for the dash-double-dotted curve Eq. (2.5) (denoted 'our' factorization) has been employed and the long-dashed curve shows the result using directly Eq. (2.1) (denoted 'KK' formula) [16]. The two curves practically coincide and indicate furthermore that higher order corrections are essential.

We will now compute the total $\gamma^* A$ cross section using two models for higher-order rescatterings: a Schwimmer unitarization [24] which is obtained from a summation of fan-diagrams with triple-Pomeron interactions and a quasi-eikonal unitarization. Nuclear shadowing is studied in terms of the ratios of cross sections per nucleon for different nuclei, defined as

$$R(A/B) \;=\; \frac{B}{A}\,\frac{\sigma_{\gamma^* A}}{\sigma_{\gamma^* B}}\,, \tag{2.7}$$

as a function of $x$, which can in turn be expressed via structure functions of the different nuclei. The simplest case is B=N, then

$$R_g^{Sch}\,(A/N)\,(x) \;=\; \int \mathrm{d}^2 b\, \frac{T_A(b)}{1+(A-1)\,f(x,Q^2)T_A(b)} \tag{2.8}$$

$$R_g^{eik}\,(A/N)\,(x) \;=\; \int \mathrm{d}^2 b\, \frac{1}{2(A-1)\,f(x,Q^2)}\,\left\{1-\exp\left[-2(A-1)T_A(b)\,f(x,Q^2)\right]\right\} \tag{2.9}$$

for the Schwimmer and quasi-eikonal models, respectively. In Eqs. (2.8) and (2.9), $f(x,Q^2)$ is given by Eq. (2.4). Both expressions (2.8) and (2.9), expanded to the first non-trivial order, reproduce the the second order rescattering result in Eq. (2.1). The gluon shadowing ratio $R_g$ for $x < 0.1$ is

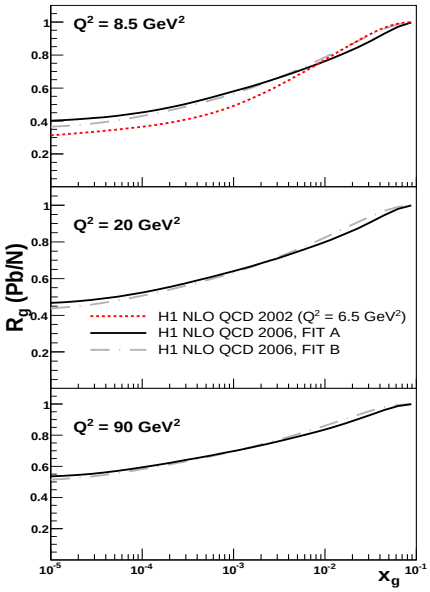


**Figure 5:** Gluon shadowing for Pb (lead) for different virtualities, $Q^2$.

shown in Fig. 4 where the calculations for Schwimmer (quasi-eikonal) model are depicted with a solid (dotted) curve.

The quasi-eikonal model gives a stronger shadowing effect than the Schwimmer model. In our framework shadowing can also be studied as a function of the impact parameter $b$, given by

$$R_g^{Sch}(A/N)(b) = \frac{1}{1+(A-1)f(x,Q^2)T_A(b)}\,, \tag{2.10}$$

$$R_g^{eik}(A/N)(b) = \frac{1}{2(A-1)T_A(b)\,f(x,Q^2)}\left\{1-\exp\left[-2(A-1)T_A(b)\,f(x,Q^2)\right]\right\}\,. \tag{2.11}$$

### 2.3 Results for gluon shadowing and validity of the model

Summing up, in the framework of the Glauber-Gribov model the total $\gamma^* A$ cross section can be calculated in a straightforward way provided the total $\gamma^* N$ cross section and the differential cross section for diffractive production are known. In what follows, calculations are made with the Schwimmer unitarization in Eq. (2.8) employing both FIT A and FIT B for the gluon density of the Pomeron.

The resulting gluon shadowing of the structure function of lead (Pb) is depicted in Fig. 5 for different virtualities, $Q^2$. The shadowing is quite strong for $x < 10^{-3}$. We note that the QCD evolution of the main term and rescattering terms are effectively treated separately in our approach, and therefore the shadowing correction has a slow, logarithmic dependence on $Q^2$ [18]. Details and further results of the calculations can be found in [26].

Equation (2.8) does not take into account anti-shadowing effects which may play an important role for $x \gtrsim 0.1$. The model for diffractive production by virtual photon described above is applicable for intermediate $Q^2 > 1-2$ GeV$^2$ [19, 20] as the parameterization of H1 data leads to a violation of unitarity for low $Q^2$ and $x \to 0$ and should be modified at very low x. This is clearly seen in

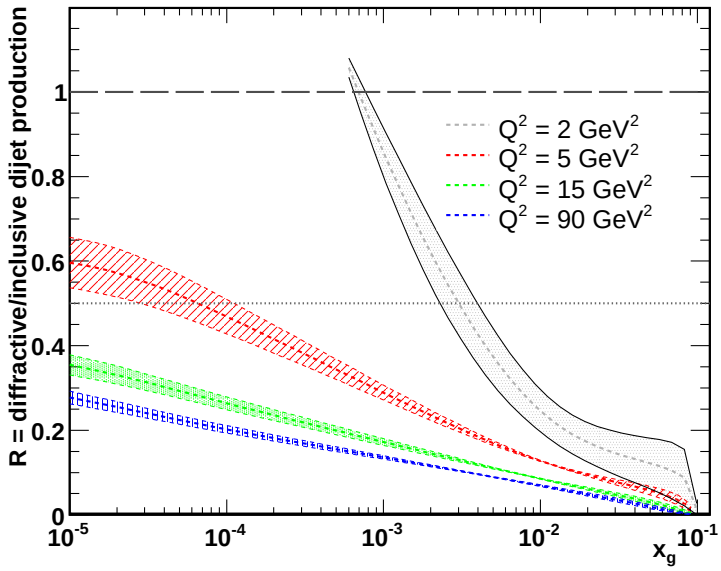


**Figure 6:** Pumplin ratio for different virtualities, $Q^2$. The shaded area denotes the uncertainty of diffractive gluon distribution function from HERA [19, 20].

Fig. 6 where we have plotted the so-called Pumplin ratio [25]

$$R = \frac{\int_x^{x_P^{max}} \mathrm{d}x_P B(x_P)\, f_P(x_P)\, \beta g^{\mathscr{D}}(\beta, Q^2)}{G_N(x, Q^2)}\,, \tag{2.12}$$

which is in fact the ratio of diffractive and inclusive dijet production. Unitarity is violated when $R \geq 1/2$. Calculations show that this takes place at low $Q^2$ and low $x$. The shaded areas in Fig. 6 represent the uncertainty in the diffractive gluon distributions from FIT A and FIT B. We conclude that our calculations are reliable in the region $x > 10^{-4}$ which is relevant for RHIC and most experiments at LHC, and should be taken with care for $x < 10^{-4}$ at low $Q^2$.

## 3. Light hadron production at SPS and RHIC

The model of gluon shadowing is now employed to study particle production in dAu collisions at RHIC energy $\sqrt{s} = 200$ GeV. There has been observed an increasing suppression of the nuclear modification factor (NMF)

$$R_{dAu}(p_\perp, \eta) = \frac{1}{\langle N_{coll}\rangle} \frac{\mathrm{d}^2 N^{dAu}/\mathrm{d}p_\perp \mathrm{d}\eta}{\mathrm{d}^2 N^{pp}_{inel}/\mathrm{d}p_\perp \mathrm{d}\eta} \tag{3.1}$$

with increasing pseudorapidity for charged particles [12]. We will not consider the effect of $p_\perp$-broadening, or Cronin effect [27], at the moment, but rather study the $\eta$ dependence of suppression. We assume, that in the ratio of forward to mid-rapidity nuclear modification factor

$$\tilde{R} = \frac{R_{dAu}(p_\perp, \eta)}{R^{norm}_{dAu}(p_\perp, 0)} \tag{3.2}$$

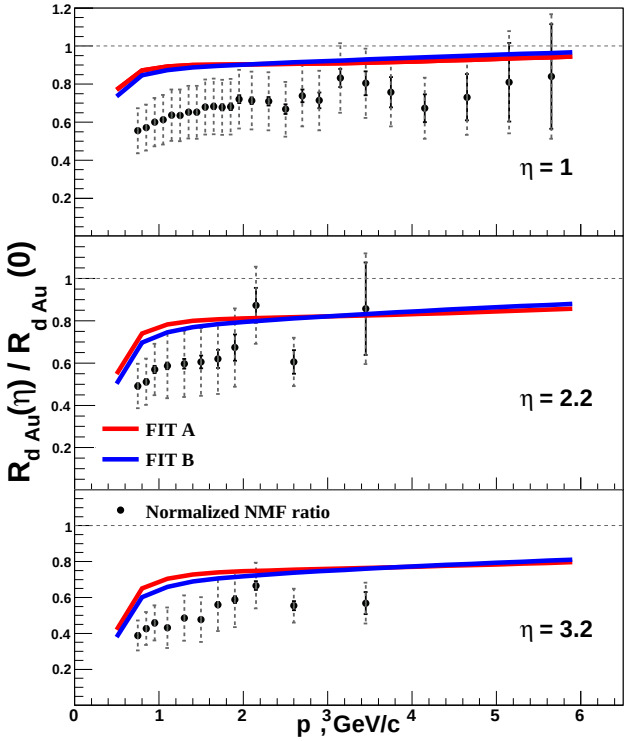


**Figure 7:** Ratio of forward and mid-rapidity nuclear modification factor. Gluon shadowing contribution to the suppression in $\eta$ is depicted for two fits of diffractive gluon density. Data is taken from [12].

the Cronin effect is cancelled out (at this energy the effect is $< 15\%$). In Eq. (3.2), $R^{norm}_{dAu}$ is the nuclear modification factor at mid-rapidity divided by our calculations of gluon shadowing. The relation of kinematical variables is given by the standard formula

$$x = \frac{cp_\perp}{\sqrt{s}} e^{-\eta} \,, \tag{3.3}$$

where $c \sim 3$. In Fig. 7 we see that gluon shadowing contribute to the suppression of the nuclear modification factor at forward rapidities, but is not sufficiently strong to describe the data quantitatively. Equation (3.3) describes *de facto* mono-jet production. The mean Bjorken x involved in particle production calculated within perturbative QCD, which describes $2 \to 2$ particle collisions or so-called two-jet kinematics, is almost two orders of magnitude larger [28]. In this case, the effect of shadowing on the suppression in Fig. 7 would be strongly reduced.

So far we have neglected a very important part of the nuclear suppression mechanism, namely the conservation of energy-momentum. This mechanism is responsible for the observed shape of $\alpha(x_F)$ in the forward region as seen in Fig. 3. Energy-momentum conservation affects the AGK cutting rules at finite energies [29] and results in an additional suppression factor [8, 11] corresponding to the substitution

$$T_A(b) \;\longrightarrow\; T_A(b) \exp\left\{-\sigma^{eff}_{hN}(x_+, p_\perp) A T_A(b)\right\} \tag{3.4}$$

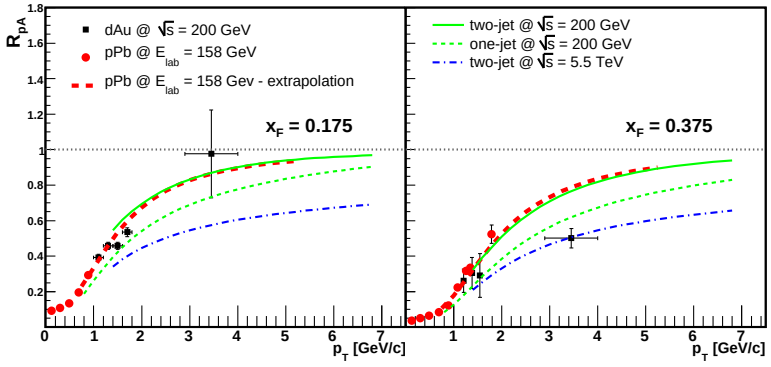


**Figure 8:** Comparison of nuclear suppression from pPb collisions at $\sqrt{s} = 17.3$ GeV (red points) [30], and dAu collisions at $\sqrt{s} = 200$ GeV (black points) [12, 31], for two values of fixed $x_F$. Red curve is extrapolation of low-energy suppression to high $p_\perp$, green curve denotes the combined effect of shadowing and energy-momentum conservation at RHIC (solid: one-jet kinematics, dashed: two-jet kinematics). We present also predictions for pPb collisions at LHC energy (dash-dotted line).

in the numerator of Eq. (2.8). The shape of $\sigma_{hN}^{eff}$ was formulated to describe data on low-$p_\perp$ nuclear modification factor for pPb collisions at SPS energy $\sqrt{s} = 17.3$ GeV [30], namely

$$\sigma_{hN}^{eff}(x_+, p_\perp) \;=\; \frac{\sigma_0 x_+}{p_\perp^2 + p_0^2}\,, \tag{3.5}$$

and $x_+ = 0.5\,(\sqrt{x_F^2 + 4m_\perp^2/s} + x_F)$ where $m_\perp$ is the transverse mass of the produced particle. Once the two free parameters, $\sigma_0$ and $p_0$, are fitted to data at $x_F = 0$, Eq. (3.4) describe the SPS nuclear modification factor for $0 < x_F \leq 0.4$. The same parameter values are also taken in the calculations of the suppression at RHIC.

A comparison of SPS [30] (red circles) and RHIC [12, 31] (black squares) data on nuclear suppression in pA collisions at $x_F = 0.175$ and $x_F = 0.375$ together with calculations of the combined effect of energy-momentum conservation and gluon shadowing is presented in Fig. 8. The red dotted curve is an extrapolation of low-energy data to higher $p_\perp$ using Eq. (3.4). The green dashed curve show calculations using Eq. (3.3) for one-jet kinematics. We have also calculated nuclear effects at RHIC using the mean Bjorken $x$ of a parton in the nucleus calculated within pQCD (solid green curve in Fig. 8). Predictions for LHC are given as well (dash-dotted curves).

The most striking fact is that data at both energies seem to overlap. This indicates that a common mechanism dominate the suppression at forward rapidities at both top SPS and top RHIC energies. Moreover, since $\sigma_{hN}^{eff}(x_+ = 0)$ decrease with energy, RHIC data gives room for an additional small shadowing contribution. Unfortunately, our model give no information about the kinematics of particle production at low and moderate $p_\perp$, and so the 'one-jet' and 'two-jet' curves indicate the total uncertainty of the model. At high-$p_\perp$, 'two-jet' kinematics is theoretically more justified.

## 4. Nuclear effects in heavy quarkonium production

Production of heavy state, such as Drell-Yan and heavy-flavor, give additional information on

the energy dependence of nuclear suppression mechanisms. Since leptons interact very weakly with the nuclear medium, Drell-Yan production holds information about the initial state effects in pA collisions, e. g. shadowing. On the other hand, hidden heavy-flavor is believed to interact quite strongly with the surrounding medium, either partonic or hadronic. Recently, the substantial decrease of the nuclear absorption in $J/\psi$ production in hA collisions between SPS energies, with $\sigma_{abs} \sim 4$ mb [32], and RHIC energies, with $\sigma_{abs} \sim 1-2$ mb [13], has attracted a lot of attention as it is in contradiction with the expectations of several theoretical models [9, 35]. In what follows, we shall show that the apparent observation of the reduction of $\sigma_{abs}$ can be interpreted as a signal of the onset of coherent scattering for heavy state production.

For heavy states the mass of the heavy system, $M_{Q\bar{Q}}$, introduces a new critical energy scale

$$s_M \;=\; \frac{M^2_{Q\bar{Q}}}{x_+}\,\frac{R_A m_N}{\sqrt{3}}\;, \tag{4.1}$$

It was shown in Ref. [11] that AGK cutting rules are changed at $s = s_M$. At energies below $s_M$ longitudinally ordered rescattering of the heavy system takes place and the produced heavy system is subject to nuclear absorption. In this energy interval Drell-Yan production does not experience nuclear suppression. At $s > s_M$ the heavy state in the projectile, which also includes light degrees of freedom, scatters coherently off nucleons of a nucleus and the conventional treatment of nuclear absorption is not adequate. For $x_F$ close to zero (central rapidity region) values of $s_M$ for $J/\psi$ and $\Upsilon$ belong to the RHIC energy region. In this kinematical region the effects of shadowing of nuclear partons become important. A similar approach for the description of $J/\psi$-suppression in dAu collisions at RHIC has been considered in Ref. [33]. For $x_F \sim 1$ the high-energy regime corresponds to an interaction with a nucleus of the fluctuation of a projectile, containing heavy quarks (of the type of "intrinsic charm" mechanism of Refs. [10, 34]).

Thus at energies $s < s_M$ the inclusive cross section for production of particle $a$ in a hA collision is given by

$$E\,\frac{\mathrm{d}^3\sigma^a_{hA}}{\mathrm{d}^3p}\,(x_+) \;=\; E\,\frac{\mathrm{d}^3\sigma^a_{hN}}{\mathrm{d}^3p}\,(x_+)\int \mathrm{d}^2b\,\frac{1-\exp\left[-\xi\,(x_+)\sigma_{Q\bar{Q}}AT_A(b)\right]}{\xi\,(x_+)\sigma_{Q\bar{Q}}}\,R^{Sch}_g\,(b,x_+,p_\perp)\;, \tag{4.2}$$

where $R^{Sch}_g$ is the $b$-dependent shadowing factor calculated in Eq. (2.10) and $\xi\,(x_+) = (1-\varepsilon)+\varepsilon x_+^\gamma$ determines the $x_+$ dependence of absorption. The suppression is concentrated at much higher $x_F$ for $Q\bar{Q}$ production than for the light hadrons because of the large mass of the $Q\bar{Q}$ system, e. g. $\gamma = 2$ for $J/\psi$ and $\gamma \sim 3$ for $\Upsilon$ production. Equation (4.2) gives a good description of experimental data on charmonium production in pA collisions at $E_{LAB} \lesssim 800$ GeV/c with $\sigma_{Q\bar{Q}} = 20$ mb and $\varepsilon = 0.75$ [11]. This corresponds to an absorption cross section of $\sigma_{abs} = 5$ mb. Note that $\sigma_{Q\bar{Q}}$ is rather large, indicating that the $c\bar{c}$ pair is produced in the color octet state rather than in the colorless state. It can also be viewed as a $D\bar{D}$ ($D^*\bar{D}^*$) system.

Equation (4.2) is not valid at asymptotic energies as the assumption of longitudinal ordering leading to it is only valid at $s < s_M$. For energies higher than $s_M$ the expression will change due to the correct treatment of coherence effects [35]

$$\frac{1-\exp\left[-\xi\,(x_+)\sigma_{Q\bar{Q}}AT_A(b)\right]}{\xi\,(x_+)\sigma_{Q\bar{Q}}} \;\longrightarrow\; AT_A(b)\exp\left(-\sigma^{eff}_{Q\bar{Q}}(x_F)\,AT_A(b)/2\right)\;, \tag{4.3}$$

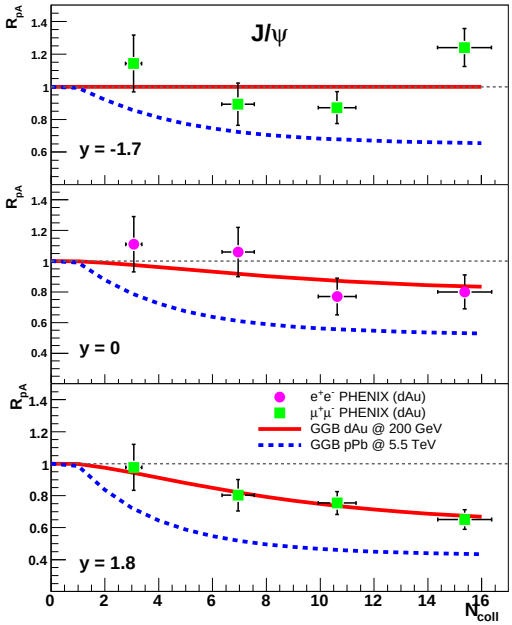


**Figure 9:** Centrality dependence of the nuclear modification factor in dAu (pPb) collisions at $\sqrt{s} = 200$ GeV (5.5 TeV) for $J/\psi$ at different rapidities. Data are taken from [13].

which is similar to the energy-momentum conservation effect for light quarks. In the model of Ref. [35], $\sigma_{Q\bar{Q}}^{eff}$ was found to be the $Q\bar{Q} - N$ total cross section.

We would like to argue that this leads to an incorrect behaviour at high energies, and propose an alternative procedure. Considering non-enhanced, Glauber-type diagrams the effective cross section $\sigma_{Q\bar{Q}}^{eff}$ should be proportional to $x_+^\gamma$, thus satisfying AGK cancellation in this limit. It was shown in Ref. [11] that at $x_F \sim 1$ the second rescattering in the low and high energy limits should coincide. This means that $\sigma_{Q\bar{Q}}^{eff} \approx \varepsilon x_+^\gamma \sigma_{Q\bar{Q}}$. Experiment on $J/\psi$ production in dAu collisions at RHIC [13] was performed in the central rapidity region, where $x_+ \sim 0.025 - 0.05$ and $\sigma_{Q\bar{Q}}^{eff}$ is therefore very small. This favors the pure nuclear shadowing scenario, which means that we do not include contributions from non-enhanced, Glauber-type diagrams.

Results of our calculations for $J/\psi$ and $\Upsilon$ production in dAu collisions at RHIC are shown in Figs. 9 and 10 together with data from [13] (solid curves). Both the centrality and the rapidity dependence of the data is well reproduced. We predict a stronger shadowing effect in pPb collisions at LHC energy $\sqrt{s} = 5.5$ TeV, which is given by the dashed curves in Figs. 9 and 10. This effect should also be taken into account when modeling nucleus-nucleus collisions at high energy.

## 5. Conclusions

We have calculated gluon shadowing in the Glauber-Gribov model using latest parameterization of diffractive gluon distribution from HERA. A strong shadowing effect is found. Our model is applicable for $Q^2 > 2$ GeV$^2$ and $10^-5 < x < 0.1$, well suited for analysis of moderate and high-$p_\perp$ particle as well as heavy-flavor production at high-energy experiments.

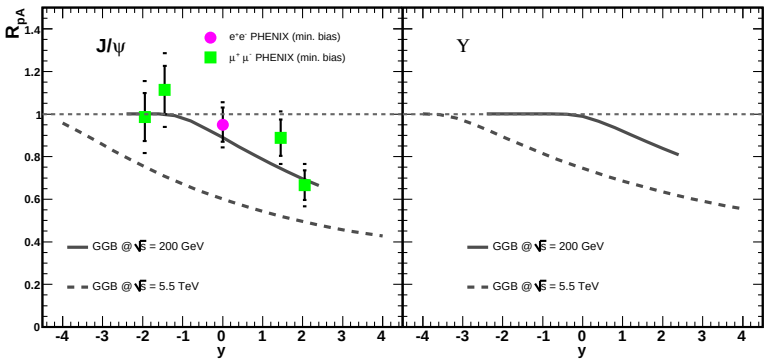


**Figure 10:** Rapidity dependence of the nuclear modification factor in min. bias dAu collisions (pPb) at $\sqrt{s} = 200$ GeV (5.5 TeV) for $J/\psi$ and $\Upsilon$ at different rapidities. Data are taken from [13].

Particle production at RHIC is dominated by coherent production both for light and heavy particles at low and moderate $p_\perp$. This is most clearly observed at mid-rapidity where $\alpha(x_F = 0)$ is below but close to unity for both charged particles and $J/\psi$ - the small suppression is solely due to gluon shadowing. Shadowing effects are stronger for light than for heavy particles as expected.

Both centrality and rapidity dependence of $J/\psi$ production in dAu collisions at RHIC have been described with our model. Even so, gluon shadowing alone cannot explain the $\eta$ dependent suppression of light particles measured at RHIC. At forward rapidities energy-momentum conservation comes into play and contributes strongly to the observed suppression. This happens more rapidly for light particle production, for $J/\psi$ and $\Upsilon$ this effect is shifted to larger values of $x_F$ due to the large mass. The combined effect of energy-momentum conservation and gluon shadowing shows good agreement with SPS and RHIC data.

The discussion of mid-rapidity nuclear modification factor is out of scope of this paper. A detailed calculation with the above mentioned effects and Cronin effect should be performed at all rapidities to draw quantitative conclusions from experimental data. Gluon shadowing by itself can also be checked against dilepton or direct photon data, and also in ultra-peripheral heavy-ion collisions.

## Acknowledgments

The authors would like to thank N. Armesto, K. Boreskov, V. Guzey, D. Röhrich and M. Strikman for interesting discussions, and B. Boimska for providing experimental data. This work was supported by the Norwegian Research Council (NFR) under contract No. 166727/V30, QUOTA-program, RFBF-06-02-17912, RFBF-06-02-72041-MNTI, INTAS 05-103-7515, grant of leading scientific schools 845.2006.2 and support of Federal Agency on Atomic Energy of Russia.

## References

[1] R. J. Glauber, *Lectures in Theoretical Physics*, Ed. W. E. Britten, Interscience Publ., N. Y., 1959, Vol. **1**, p.315

[2] S. Mandelstam, *Cuts in the angular momentum plane. 2*, *Nuovo Cim.* **30** (1963) 1148

[3] V. N. Gribov, *Glauber corrections and the interaction between high-energy hadrons and nuclei*, *Sov. Phys. JETP* **29** (1969) 483

[4] V. N. Gribov, *Interaction of gamma quanta and electrons with nuclei at high-energies*, *Sov. Phys. JETP* **30** (1970) 709

[5] D. M. Alde *et al.*, *A dependence of $J/\psi$ and $\psi'$ production at 800 GeV/c*, *Phys. Rev. Lett.* **66** (1991) 133

[6] M. J. Leitch *et al.*, *Measurement of Differences between $J/\psi$ and $\psi'$ Suppression in p-A Collisions*, *Phys. Rev. Lett.* **84** (2000) 3256

[7] NA50 Collaboration, R. Shahoyan *et al.*, *New results on nuclear dependence of $J/\psi$ and $\psi'$ production in 450-GeV pA collisions*, hep-ex/0207014

[8] B. Z. Kopeliovich, J. Nemchik, I. K. Potashnikova, M. B. Johnson and I. Schmidt, *Breakdown of QCD factorization at large Feynman x*, *Phys. Rev. C* **72** (2005) 054606

[9] B. Kopeliovich, A. Tarasov and J. Hufner, *Coherence phenomena in charmonium production off nuclei at the energies of RHIC and LHC*, *Nucl. Phys. A* **696** (2001) 669

[10] R. Vogt, *$x_F$ dependence of $\psi$ and Drell-Yan production*, *Phys. Rev. C* **61** (2000) 035203

[11] K. Boreskov, A. Capella, A. Kaidalov and J. Tran Thanh Van, *Heavy-quark and lepton-pair production on nuclei*, *Phys. Rev. D* **47** (1993) 919

[12] BRAHMS Collaboration, I. C. Arsene *et al.*, *On the evolution of the nuclear modification factors with rapidity and centrality in d + Au collisions at $\sqrt{s}$ = 200-GeV*, *Phys. Rev. Lett.* **93** (2004) 242303

[13] PHENIX Collaboration, S. S. Adler *et al.*, *$J/\psi$ production and nuclear effects for d+Au and p+p collisions at $\sqrt{s_{NN}}$ = 200-GeV*, *Phys. Rev. Lett.* **96** (2003) 012304

[14] W. M. Geist, *Atomic mass dependence in soft and hard p A collisions*, *Nucl. Phys. A* **525** (1991) 149C, and references therein

[15] V. A. Abramovsky, V. N. Gribov and O. V. Kancheli, *Character Of Inclusive Spectra And Fluctuations Produced In Inelastic Processes By Multi - Pomeron Exchange*, *Sov. J. Nucl. Phys.* **18** (1974) 308

[16] V. A. Karmanov and L. A. Kondratyuk, *Inelastic screening for high energy nucleon scattering on complex nuclei*, *JETP Letters* **18** (1973) 451

[17] A. B. Kaidalov, *Diffractive production mechanisms*, *Phys. Rep.* **50** (1979) 157

[18] S. J. Brodsky, P. Hoyer, N. Marchal, S. Peigné and F. Sannino, *Structure functions are not parton probabilities*, *Phys. Rev. D* **65** (2002) 114025

[19] H1 Collaboration, A. Aktas *et al.*, *Measurement and QCD analysis of the diffractive deep-inelastic scattering cross-section at HERA*, *Eur. Phys. J. C* **48** (2006) 715

[20] H1 Collaboration, A. Aktas *et al.*, *Diffractive deep-inelastic scattering with a leading proton at HERA*, *Eur. Phys. J. C* **48** (2006) 749

[21] M. Mozer for the H1 Collaboration, *Diffractive di-jets and combined fits*, talk at the 14th International Workshop on Deep Inelastic Scattering, DIS 2006, Tsukuba [H1prelim-06-016]

[22] H1 Collaboration, *Measurement and NLO DGLAP QCD Interpretation of Diffractive Deep-Inelastic Scattering at HERA*, paper **980** submitted to the 31st International Conference on High Energy Physics, ICHEP 2002, Amsterdam [H1prelim-02-012]

[23] J. Pumplin, D.R. Stump, J. Huston, H.L. Lai, P. Nadolsky and W.K. Tung, *New generation of parton distributions with uncertainties from global QCD analysis*, *JHEP* **0207** (2002) 012

[24] A. Schwimmer, *Inelastic Rescattering And High-Energy Reactions On Nuclei*, *Nucl. Phys. B* **94** (1975) 445

[25] A. B. Kaidalov, V. A. Khoze, A. D. Martin and M. G. Ryskin, *Unitarity effects in hard diffraction at HERA*, *Phys. Lett. B* **567** (2003) 61

[26] K. Tywoniuk, I. C. Arsene, L. Bravina, A. Kaidalov and E. Zabrodin, *Gluon shadowing in the Glauber-Gribov model at HERA*, arXiv:0705.1596[hep-ph]

[27] J. W. Cronin *et al.*, *Production of Hadrons with Large Transverse Momentum at 200-GeV, 300-GeV, and 400-GeV*, *Phys. Rev. D* **11** (1975) 3105

[28] V. Guzey, M. Strikman and W. Vogelsang, *Observations on dA scattering at forward rapidities*, *Phys. Lett. B* **603** (2004) 173

[29] A. Capella and A. Kaidalov, *Hadron-hadron and hadron-nucleus scattering in reggeon calculus with energy-momentum conservation*, *Nucl. Phys. B* **111** (1976) 477

[30] B. Boimska, Ph. D. Dissertation (Warsaw 2004), CERN-THESIS-2004-035

[31] STAR Collaboration, L. S. Barnby *et al.*, *Identified particle dependence of nuclear modification factors in d+Au collisions at RHIC*, *J. Phys. G* **30** (2004) S1121, [nucl-ex/0404027]

[32] NA50 Collaboration, L. Ramello *et al.*, *Charmonia absorption in p A collisions at the CERN SPS: Results and implications for Pb Pb interactions*, *Nucl. Phys. A* **715** (2003) 243c

[33] A. Capella and E. G. Ferreiro, *Why does the J/psi nuclear absorption decrease with increasing energy?*, hep-ph/0610313

[34] S. J. Brodsky and P. Hoyer, *The Intrinsic Charm of the Proton*, *Phys. Lett. B* **93** (1980) 451

[35] M. A. Braun, C. Pajares, C. A. Salgado, N. Armesto and A. Capella, *Probabilistic versus field theoretical description of heavy flavor production off nuclei*, *Nucl. Phys. B* **509** (1998) 357